Metallomics

PAPER

View Article Online
View Journal | View Issue

Cite this: *Metallomics*, 2020, **12**, 371

Brake dust exposure exacerbates inflammation and transiently compromises phagocytosis in macrophages†

Liza Selley, ‡*[a] Linda Schuster,‡[bc] Helene Marbach,[b] Theresa Forsthuber,[b] Ben Forbes,[b] Timothy W. Gant,[de] Thomas Sandström,[f] Nuria Camiña,[g] Toby J. Athersuch,[eh] Ian Mudway[gi] and Abhinav Kumar[b]

Studies have emphasised the importance of combustion-derived particles in eliciting adverse health effects, especially those produced by diesel vehicles. In contrast, few investigations have explored the potential toxicity of particles derived from tyre and brake wear, despite their significant contributions to total roadside particulate mass. The objective of this study was to compare the relative toxicity of compositionally distinct brake abrasion dust (BAD) and diesel exhaust particles (DEP) in a cellular model that is relevant to human airways. Although BAD contained considerably more metals/metalloids than DEP (as determined by inductively coupled plasma mass spectrometry) similar toxicological profiles were observed in U937 monocyte-derived macrophages following 24 h exposures to 4–25 μg ml^{-1} doses of either particle type. Responses to the particles were characterised by dose-dependent decreases in mitochondrial depolarisation ($p \leq 0.001$), increased secretion of IL-8, IL-10 and TNF-α ($p \leq 0.05$ to $p \leq 0.001$) and decreased phagocytosis of *S. aureus* ($p \leq 0.001$). This phagocytic deficit recovered, and the inflammatory response resolved when challenged cells were incubated for a further 24 h in particle-free media. These responses were abrogated by metal chelation using desferroxamine. At minimally cytotoxic doses both DEP and BAD perturbed bacterial clearance and promoted inflammatory responses in U937 cells with similar potency. These data emphasise the requirement to consider contributions of abrasion particles to traffic-related clinical health effects.

Received 10th October 2019,
Accepted 6th December 2019

DOI: 10.1039/c9mt00253g

rsc.li/metallomics

Significance to metallomics

Metal/metalloid content is consistently associated with the capacity of tailpipe-derived particulates to cause cellular stress and inflammation in the airways. Here, we demonstrate that exposure to brake dust (a richly metallic, non-tailpipe-derived, wear particle) also impairs the ability of immune cells to ingest respiratory pathogens and enhances inflammatory signalling in a transient but metal-dependent manner.

Introduction

Residential proximity to roads, particularly those carrying high proportions of diesel traffic, has been associated with increased mortality rates, exacerbations of respiratory disease, increased cardiovascular symptoms[1] and adverse impacts on lung development and cognition in children.[2,3] Traffic-derived pollution represents a heterogeneous mixture of gases and particulates,

[a] *MRC Toxicology Unit, University of Cambridge, Hodgkin Building, Lancaster Road, Leicester, LE1 9HN, UK. E-mail: ls802@mrc-tox.cam.ac.uk*
[b] *Institute of Pharmaceutical Science, Faculty of Life Sciences and Medicine, King's College London, London, SE1 9NH, UK. E-mail: helenemarbach@gmx.de, a1107500@unet.univie.ac.at, ben.forbes@kcl.ac.uk, notabhinav@gmail.com*
[c] *German Cancer Research Center (DKFZ) & Bioquant Center, Division of Chromatin Networks, 69120, Heidelberg, Germany. E-mail: linda.schuster@dkfz-heidelberg.de*
[d] *Department of Toxicology, Centre for Radiation, Chemical and Environmental Hazards, Public Health England, OX11 0RQ, UK. E-mail: tim.gant@phe.gov.uk*
[e] *MRC-PHE Centre for Environment and Health, Imperial College, London, W2 1PG, UK. E-mail: toby.athersuch@imperial.ac.uk*
[f] *Department of Public Health and Clinical Medicine, Division of Medicine, Umeå University, Umeå, Sweden. E-mail: thomas.sandstrom@umu.se*
[g] *MRC-PHE Centre for Environment and Health, King's College London, London, SE1 9NH, UK. E-mail: nuria.camina@kcl.ac.uk, ian.mudway@kcl.ac.uk*
[h] *Department of Surgery and Cancer, Faculty of Medicine, Imperial College London, London, SW7 2AZ, UK*
[i] *Department of Analytical and Environmental Sciences, Faculty of Life Sciences and Medicine, King's College London, London, SE1 9NH, UK*

† Electronic supplementary information (ESI) available. See DOI: 10.1039/c9mt00253g

‡ Denotes equal contribution to authorship.

produced by fuel combustion and lubricant volatilisation, wear of mechanical components and abrasion of the road surface.[4]

To date, diesel exhaust has been the major focus of investigations into traffic-derived particulate toxicity. This focus has been supported by epidemiological studies which demonstrate significant associations between adverse health outcomes/endpoints and tracers of diesel tailpipe emissions.[5,6] Additionally, concurrent *in vitro* and *in vivo* experimentation has demonstrated the capacity of diesel exhaust particles (DEP) to stimulate xenobiotic and antioxidant defences, redox-sensitive signalling pathways, inflammatory cascades and the activation of airway nerve fibres.[7–10] In contrast, the toxic potential of non-tailpipe particulates, such as those produced by brake, tyre or clutch wear has received little attention.

Brake abrasion dust (BAD) is the most abundant non-tailpipe particulate measured in urban areas,[11,12] contributing up to 55% of non-tailpipe PM_{10}[13] and 21% of total traffic PM_{10},[14] with the contribution forecast to increase relative to tailpipe PM, as emission regulations for diesel vehicles tighten.[4] Often portrayed as coarse mode PM, abrasion-derived particles also exist within the respirable fine and ultrafine fractions[15] giving them potential to penetrate the distal lung, deposit in respiratory tract lining fluids (RTLFs) and interact with resident phagocytes and epithelial cells. Unlike tailpipe-derived particles, BAD is rich in metals,[4] many of which (*e.g.* Fe and Cu) can catalyse the formation of reactive oxygen species (ROS) within the oxygen-rich conditions of the RTLFs, thus challenging the high concentrations of low molecular weight antioxidants (glutathione, urate and α-tocopherol), antioxidant enzymes (superoxide dismutase and catalase) and metal-binding proteins (transferrin and caeruloplasmin), which exist to protect the epithelial surface from oxidative attack.[16] Indeed, within cell-free systems, BAD displays greater capacity to elicit damaging oxidation reactions than DEP.[17]

Despite associations existing between occupational metal fume exposures and inflammatory pulmonary pathophysiologies (including metal fume fever which has been recognised since the 1950's),[18] very few publications have explored the direct adverse effects of BAD exposure in pulmonary models. Employing mechanistic understanding of how such occupational pathophysiologies develop,[18] those that have, focus predominantly on the pro-inflammatory and oxidative stress-inducing potential of the particles. Mimicking exposure of the alveolar epithelium, Gasser *et al.* demonstrated that the metallic fraction of BAD induces pro-inflammatory signalling and disrupts tight junction integrity in A549 cells.[19] A comparatively reduced inflammatory response was documented in Calu-3 bronchial epithelial cells following exposure to Fe and Cu-rich BAD, but increases in IL-6 secretion did associate with ROS production following exposure to concentrations greater than 50 μg cm^{-2}.[20] Using a mouse inhalation model, Gerlofs-Nijland *et al.* found that the fine fraction of BAD also induced pro-inflammatory responses *in vivo* following acute (1.5–6 h) exposures of up to 9 mg m^{-3}. Based upon influx of circulating immune cells (polymorphonucleocytes) and concentrations of cytokines secreted into the bronchiolar lavage fluid (BALF) by these and by resident airway phagocytes and epithelial cells, the authors found that particles produced by low and semi-metallic brake pads induced pulmonary inflammation at a similar dose to DEP and tyre wear, but exhibited lower potency than particles produced through biomass combustion. BAD produced from non-asbestos organic (NAO) brake pads was found to be the most potent of all particles tested: a result that the authors attribute to its high copper content.[21]

Other studies have attributed toxicological endpoints to BAD and general abrasion-related particles by examining the toxicity of roadside PM, with and without the use of metal chelators to try and isolate the metal-dependent signature. Using this approach, the metal content of roadside PM in samples collected throughout Europe was shown to be related to the capacity of RAW264.7 monocyte-derived macrophages (MDM) to release arachidonic acid metabolites.[22] Other within-city and pan-national studies have shown that the capacity of ambient PM to elicit damaging oxidation reactions is strongly related to their content of brake-wear related metals, such as Cu, Ba and Sb.[23–25] Susceptibility to pulmonary infections remains unexamined in the context of BAD exposure, but exposure to metal-rich aerosols (especially those containing Fe, Cr, Al and Ti) has been associated with increased mortality from pneumonia in welders and foundry workers,[26,27] enhance pneumococcal adhesion to airway epithelial cells,[32] and impairment of bacterial phagocytosis in airway phagocytes.[36,37] Given the metallic, Fe-rich composition of BAD, it is therefore possible that these and other metal-rich vehicle-derived particles could contribute to the heightened incidence of pulmonary infections that exists in urban environments.[30,31]

In the current study, we used the U937 monocyte-derived macrophage cell line to perform side-by-side characterisations of the toxicity that BAD and diesel exhaust particles exert on airway macrophages (phagocytes found resident to the alveolar lumen surface during homeostasis). The work explored endpoints additional to inflammatory potential that had previously been shown to be perturbed by diesel particulate challenge: mitochondrial dysfunction, cell morphometry as an indicator of apoptosis or necrosis and phagocytic competence. We hypothesised that both particle types would perturb cell function, but that there would be significant differences in response, reflecting the marked compositional difference between the particle species.

Methods

Materials

SRM-2975 DEPs were purchased from National Institute of Standards and Technology and mixed BAD sample was extracted from a bag filter taken from the ventilation duct of the SMP Svensk Maskinprovning machinery testing plant (Långsele, Sweden). The filter contained a yearly collection of abrasion dusts collected from drum brakes that are used in buses and trucks in Europe (and elsewhere) and produced under conditions representative of urban driving and high-speed braking conditions (ESI,† File 1). Unless stated, other materials were sourced from Sigma Aldrich (USA).

Particle size measurement using dynamic light scattering (DLS)

The hydrodynamic diameter of 14 μg ml^{-1} BAD and SRM-2975 in culture media (without phenol red) was measured after 0, 4 and 24 h of incubation at 37 °C in humidified 5% CO_2, 95% atmospheric air (standard conditions). Particle size was measured using a Malvern Zetasizer Nano ZS (Malvern Instruments, UK) at a temperature of 25 °C. Each sample was measured over 3 runs with each run consisting of 6 individual readings.

Visual assessment of particles using scanning electron microscopy (SEM)

BAD (collected after methanol extraction and prior to suspension in PBS) were gold plated using an EMITECH K550 sputter coater and imaged using a FEI Quanta200 Emission Scanning Electron Microscope (Field Electron and Ion Company, USA).

Quantification of metals/metalloids in PM samples and biological matrices by inductively coupled plasma mass spectrometry (ICP-MS)

The metal/metalloid content of BAD, SRM-2975 and cell lysates was characterised by ICP-MS. Cell lysates were collected by washing the monolayer 3× in PBS then rocking for 1 h in ultrapure chelex-100 treated H_2O. All PM samples and cell lysates were taken through an identical digestion protocol, as PM was visible in the material recovered from the cell challenges. 100 μl of PM suspension (50 μg ml^{-1} solutions of BAD and SRM 2975 prepared in ultrapure chelex-100 treated H_2O) or cell lysate was added to 0.9 ml of aqua regia (1 : 3 HNO_3 (60%) : HCL (30%), both Ultrapure grade, from Merck, UK). After addition of 70 μl of Yttrium (stock solution, 1 ppm, SCP Science, France) as an internal standard (I.S.), samples were mixed and incubated for 90 minutes at 100 °C. Blank digestions were performed with 1 ml chelex-100 treated H_2O spiked with the I.S. After cooling to room temperature, the digests were diluted with 6 ml chelex-100 treated H_2O. Samples were then transferred to the Mass Spectroscopy Unit at King's College London for the quantification of Al (isotope 27; natural abundance 100%), As (75; 100%), Ba (135; 6.95%), Cu (63; 69.17%), Fe (56; 91.75%), Mn (55; 100%), Mo (95; 15.92%), Ni (60; 26.22%), Cr (52; 83.79%), V (51; 99.75%), Sb (121; 57.21%), Zn (66; 27.90%), Cd (111; 12.80%), Ti (47; 7.44%), Ca (44; 2.08%), W (184; 30.64%), Sn (118; 24.22%) and Y (89; 100%) by ICP-MS using a NexION 350D ICP-MS (PerkinElmer, UK). Elemental concentrations were determined with reference to a 6-point standard curve based on an ICP multi element standard solution VI CertiPUR (Merck, Lot. No. OC529648). Antimony which is not present in this multi-elemental standard was analysed against its own standard curve (Antimony ICP standard, MERCK). Determined concentrations represent the mean of 5 individual injections with the final values corrected for the background elemental concentrations determined in the chelex-100 treated water blanks which was run in parallel to each batch of samples and corrected for variation in the I.S. The following elements were analysed using the dynamic reaction cell to prevent know polyatomic interferences: Al, As, Ma, V, Cr, Cu, Ni, Zn, Ca and Fe. All cell lysate concentrations were normalised to total protein concentrations. To prevent contamination of the samples by atmospheric fall out, all sample digestions and pre-treatment steps were performed in an extracted laminar flow cabinet and analysis by ICP-MS was performed within the Clean Room at the London Metallomics faculty at King's College London. All digestion tubes (Elkay, Basingstoke, UK), 15 ml non pigmented tube and caps (Elkay) and pipette tips were pre-washed in 5% HNO_3, followed by rinsing three times in Chelex-100 resin treated ultra-pure water prior to use.

Measurement of particulate oxidative potential

The oxidative potential of BAD and SRM-2975 samples was established by quantifying the capacity of the particles to deplete ascorbate and glutathione from a synthetic RTLF that is formulated to contain *in vivo*-relevant concentrations of antioxidants, surfactant proteins and immunoglobulins.[34] After incubating the particles with the RTLF for 4 h (pH 7.0, 37 °C) at a concentration of 50 μg particles per ml RTLF, samples of the particle-RTLF mixture were assayed for ascorbate concentrations using reverse-phase high performance liquid chromatography and glutathione disulphide/total glutathione concentrations using a GSSG-reductase-DNTB recycling assay. The details of these methods and handling of the resulting data have been described previously by Mudway *et al.*[33]

U937 culture and differentiation

U937 monocytes were cultured at 37 °C in 5% CO_2, 95% atmospheric oxygen (standard conditions) in RPMI 1640 medium supplemented with 10% foetal bovine serum, 1% L-glutamine and 1% penicillin–streptomycin (culture medium (CM)). Cells were seeded at densities of 1 × 10^6 and 1.25 × 10^5 cells in 12 and 96 well plates (respectively) in CM containing 4 nM phorbol 12-myristate 13-acetate (PMA) to encourage differentiation into adherent macrophages. Cells were cultured in the presence of PMA for 96 h then rested in CM for 24 h before experimentation.

Particle exposure

1 mg ml^{-1} stocks of BAD and SRM-2975 (in PBS) were sonicated for 2 minutes at 70 Hz and diluted to 4–25 μg ml^{-1} in CM. Particles were applied to cells in 1 ml and 200 μl volumes for 12 and 96 well plates (respectively) and incubated for 4–48 h under standard conditions. Even dispersion of particles was confirmed using light microscopy. For cytokine secretion and phagocytosis assays, cells were also exposed to 1 μg ml^{-1} lipopolysaccharide (LPS) or 1 μg ml^{-1} benzopyrene (a model polycyclic aromatic hydrocarbon (PAH)) or to particles in the presence of 5 μg ml^{-1} desferroxamine (DFO). Reversibility of responses was assessed by including a 24 h 'rest' incubation in particle-free medium following particle exposure but prior to assaying.

3-(4,5-Dimethylthiazol-2-yl)-2,5-diphenyl tetrazolium bromide (MTT) assay

Mitochondrial oxidoreductase activity was used as a proxy for cell viability. After exposure, cells were incubated with 2.5 μg ml^{-1}

MTT reagent in CM for 4 h. The formazan crystals that formed were dissolved in a 1 : 1 solution of 20% sodium dodecyl sulphate and dimethylformamide and were read by microplate reader (SpectraMax 190) at 570 nm. Six measurements were made per treatment.

Cellular staining and imaging

Following particle challenge, cells were incubated with 150 nM MitoTracker Red Stain (Life Technologies, MA, USA) and 12.5 nM Image It DEAD Green Viability (Life technologies) for 30 minutes at 37 °C. Cells were washed twice with PBS to remove unbound dye and were fixed with 4% paraformaldehyde for 15 minutes at room temperature. After 2 washes with PBS, cells were permeabilised with 0.1% Triton X-100 for 20 minutes at room temperature. Cells were washed twice more with PBS then incubated with 1 ng ml^{-1} HCS M Cell Mask Deep Red stain (Life Technologies) and 40.5 μM Hoechst 33342 trihydrochloride trihydrate (Life Technologies) at room temperature for 2 hours. Unbound dye was removed during 2 PBS washes. 2 mM carbonyl cyanide 4-(trifluoro-methoxy)-phenylhydrazone (Sigma) and 0.2% Triton X-100 treatments were included as positive controls for mitochondrial membrane potential disruption and cytotoxicity (respectively). Cells were imaged using an IN Cell Analyzer 6000.

Cytokine ELISAs

Supernatants were collected post-challenge and centrifuged at 16 000 × *g* for 10 minutes to remove extracellular particles. Cytokine concentrations were measured using Human IL-10, IL-8 ELISA and TNF-α Ready-SET-Go! kits (eBioscience, San Diego, CA) as instructed by the manufacturers.

Bacterial stocks

An isolated colony of *Staphylococcus aureus* (*S. aureus*) strain Newman (Edgeworth, KCL) was grown overnight at 37 °C in Mueller Hinton broth (MHB) (Oxoid, Waltham, MA). A Jenway 6300 visible range spectrophotometer was used to dilute the culture to 1 × 10^4 colony forming units ml^{-1} (CFU ml^{-1}) in MHB.

Bacterial growth assay

1 × 10^4 CFU ml^{-1} *S. aureus* were centrifuged at 5000 × *g* for 15 minutes and re-suspended in MHB broth spiked with 25 μg ml^{-1} BAD, 25 μg ml^{-1} SRM-2975 or 50 μg ml^{-1} gentamicin (as a positive control for antibacterial activity) or with 100% MHB (as a negative control). The culture was incubated for 4 h at 37 °C with 50 μl aliquots being removed and plated in duplicate every hour on MH agar (MHB supplemented with 0.01 g ml^{-1} agar). Plates were incubated overnight at 37 °C and the bacterial colonies quantified manually.

Quantification of bacterial phagocytosis behaviour

Following particulate challenge, U937s were washed 3 times with PBS and inoculated with 1 ml of the diluted *S. aureus* culture to produce a multiplicity of infection of 0.01. Plates were centrifuged at 2700 × *g* for 10 minutes to encourage contact between the bacteria and macrophages and incubated under standard conditions for 2 h. Wells were washed 3 times with PBS and treated with 50 μg ml^{-1} gentamicin for 10 minutes to remove and kill bacteria that remained extracellular to the macrophages. U937s were then lysed with sterile deionised H_2O to release internalised bacteria into the supernatant. The supernatants were diluted 1 : 10 in MHB and grown in duplicate on Mueller Hinton agar overnight under standard conditions. *S. aureus* colonies were counted manually.

Statistical analysis

Raw data were converted to percentages of particle-free control samples using Microsoft Excel and identification of significant differences between treatment types were made using GraphPad Prism Version 5.0 (Graphpad Software). Statistical assessment was conducted using one-way analysis of variance (ANOVA) for DLS, oxidative potential, MTT, ELISA, cell staining and bacterial phagocytosis assays and two-way ANOVA tests for metal chelator and bacterial growth assays. To address the increased likelihood of Type I errors by conducting multiple comparisons, *post hoc* Bonferroni corrections were performed. *P*-Values ≤ 0.05 were considered to represent statistically significant changes.

Results

Physicochemical characteristics of particles

As a standard reference material, the physicochemical properties of SRM-2975 have been characterised previously.[35,59] In contrast, the BAD sample employed here has not been studied before so required characterisation prior to use. Scanning electron microscopy identified BAD as highly polydisperse with a particle diameter range of 0.2–22.9 μm (median 2.4 μm). 51.3% of the particles fell within the $PM_{2.5}$ size fraction with the remaining 48.6% classifying as PM_{10}. The particles displayed a smooth surface texture with jagged edges evident on the larger particles only. It was notable that there was no evidence of fibres from the filter matrix in the extract (Fig. 1Ai–ii). To determine the hydrodynamic diameter of the particles when dispersed in CM, complimentary DLS experiments were performed across a 24 h time-course to assess the degree of particle agglomeration that may have occurred during experiments (Table 1). At the time of exposure, BAD had an average hydrodynamic diameter of 0.6 μm while SRM-2975 had a larger average hydrodynamic diameter of 1.2 μm. Both particles exhibited high polydispersity indices (PDI): 0.7 for BAD 0.7 for SRM-2975. The size (and heterogeneity of sizes) of both particles did not significantly alter during the experimental time-course ($p > 0.05$), suggesting that minimal agglomeration or dispersion occurred.

Average hydrodynamic diameters (±SE) and PDI (±SE) of BAD and SRM-2975 samples (14 μg ml^{-1}) ascertained using dynamic light scattering after 0, 4 or 24 h incubation in CM at 37 °C. Measurements were made at 25 °C and values were produced over 3 runs consisting of 6 readings each.

The metal/metalloid content of the particles was characterised using ICP-MS. Fourteen of the eighteen tested metal/metalloids

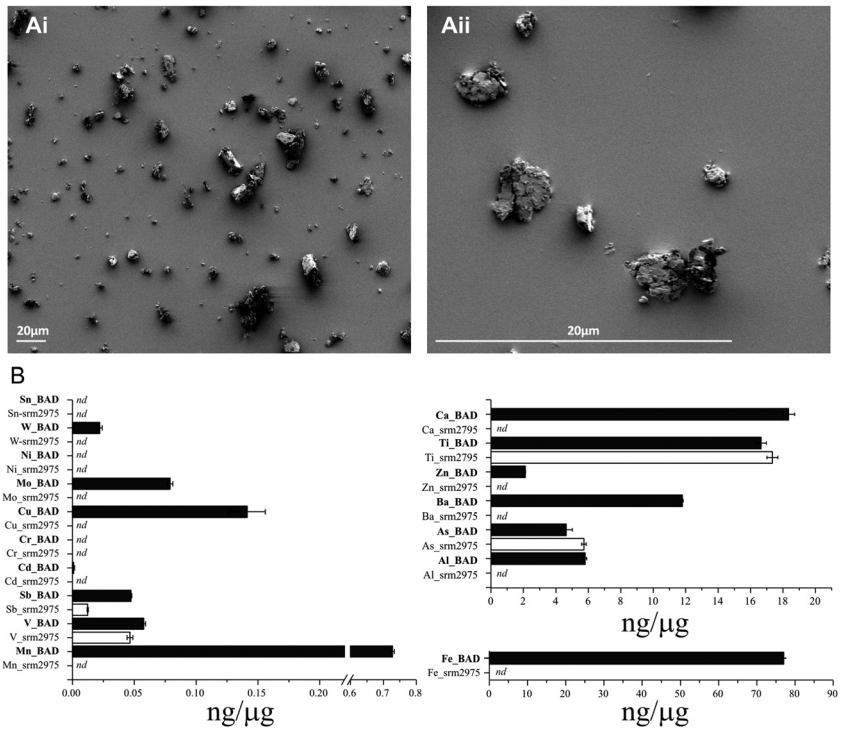

Fig. 1 Representative images and particle size distributions of BAD taken *via* SEM at 1000× and 4000× magnification (Ai–ii). Panel B illustrates the concentrations of metals/metalloids associated with BAD and DEP as determined by ICP-MS (B). Concentrations are illustrated as means ± SE based on triplicate preparations of each PM sample.

Table 1 Hydrodynamic diameter of BAD and SRM-2975 as determined by DLS

Particle	Dispersant	Time point (hours)	Average diameter (nm)	Average PDI
BAD	CM	0	610.3 ± 72.7	0.7 ± 0.1
		4	617.5 ± 119.0	0.7 ± 0.1
		24	616.2 ± 1.6	0.6 ± 0.1
SRM-2975	CM	0	1214.3 ± 108.6	0.8 ± 0.2
		4	1179.5 ± 269.4	0.9 ± 0.1
		24	1228.2 ± 115.8	0.9 ± 0.1

were detectable in BAD following subtraction of the digestion blank, with Fe (77.0 ± 0.6 ng μg^{-1}), Ca (18.3 ± 0.3 ng μg^{-1}), Ti (16.7 ± 0.3 ng μg^{-1}) and Ba (11.8 ± <0.1 ng μg^{-1}) being most abundant. The SRM-2975 was largely devoid of metals/metalloids, with only Ti (17.3 ± 0.3 ng μg^{-1}), As (5.7 ± 0.1 ng μg^{-1}), V (0.05 ± 0.0 ng μg^{-1}) and Sb (0.01 ± 0.0 ng μg^{-1}) being detected at levels significantly above baseline (digestion blank). Of these common metals, equivalent concentrations of Ti, As and V were observed in the BAD and SRM-2975 PM samples, with Sb significantly enriched in the BAD samples ($p \leq 0.001$), (Fig. 1B). Due to the contrasting content of redox-active metals in the two particles, their relative oxidative potentials were determined based on their capacity to deplete ascorbate and glutathione from a RTLF simulant containing *in vivo*-relevant concentrations of airway antioxidants.[34] Both BAD and SRM-2975 samples significantly depleted ascorbate by 44 and 55% respectively ($p \leq 0.001$, relative to particle-free controls), whilst BAD alone induced significant oxidation of glutathione (12%, $p \leq 0.05$) (ESI,† Fig. S1).

BAD and SRM-2975 are not cytotoxic to U937 macrophages

Light microscopy confirmed that U937s were capable of ingesting BAD and SRM-2975 during 24 h exposures (ESI,† Fig. S2). Consistent with this, intra-cellular concentrations of metals detected within the BAD particles were enriched in all samples challenged with the pollutant. While strongly variable in magnitude (and therefore, not explored for statistical significance), dose-dependent increases in Fe, Al and Mn content (253–2453, 48–187 and 36–100%, respectively) were visible, and 16–23, 141–431 and 510–1992% increases in As, V and Ba content were detected across the 4–14 μg ml^{-1} exposure range (respectively). Increases in cellular Ca and Cu content also occurred following 25 μg ml^{-1} exposures (261 and 107% respectively) (Fig. 2A–D). Similarly, intracellular V content increased by 34–367% where macrophages were challenged with 4–25 μg ml^{-1} SRM-2975 while As and Ti concentrations were marginally elevated in a non-dose dependent manner following exposures to 4–14 μg ml^{-1} SRM-2975 (43–50 and 22–26%, respectively) (Fig. 2E and F).

MTT assays were employed to assess the cytotoxic potential of particle-cell interactions, using mitochondrial oxidoreductase activity as a proxy for cell viability. BAD (4–25 μg ml^{-1}) caused no significant changes in signal following the 24 h exposure but SRM-2975 exposure caused dose-dependent reductions in formazan crystal formation (17–44%, $p \leq 0.001$–0.05), indicating

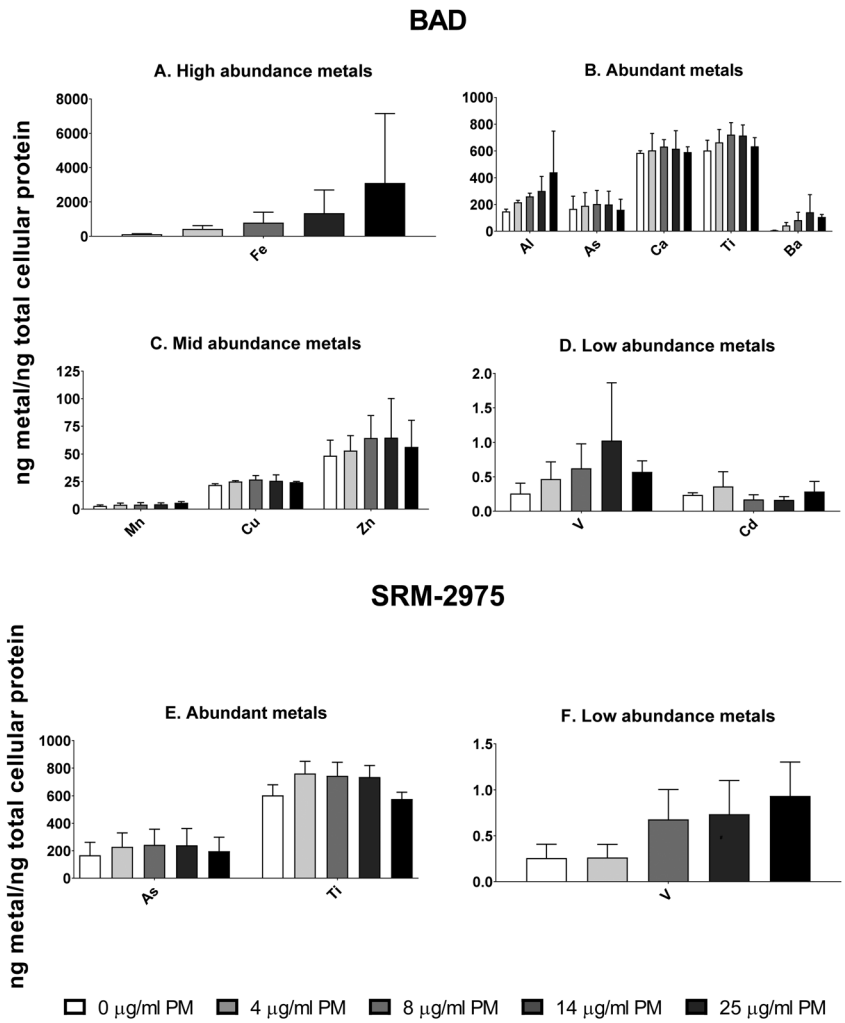

Fig. 2 Quantities of particle-associated metals/metalloids detected within the lysates of U937 following exposure to 4–25 μg ml^{-1} BAD (A–D) or SRM-2975 (E and F). Values were acquired *via* ICP-MS and normalised to total cellular protein as determined by bicinchoninic acid assay. They are displayed as the mean ± SE of 3 replicates.

a reduction in cellular activity. These SRM-2975-induced reductions in MTT signal were visible as early as 4 h post-exposure at doses ≥8 μg ml^{-1} ($p \leq 0.01$–0.05) but were not detected until 48 h post-BAD exposure where they occurred at a similar magnitude to the response induced by 24 h exposures to the DEP (19–41%, $p \leq 0.01$–0.05).

Staining with fluorescent nuclear and cytoplasmic dyes, indicated that neither particle caused changes in nuclear or cellular area (morphometric markers of apoptotic or necrotic activity) after 24 h exposure, even at the highest tested dose (25 μg ml^{-1}) (Fig. 4A–D). The cells did however, display evidence of mitochondrial dysfunction with dose-dependent decreases in the Mitotracker Red signal after BAD (7–65%) and SRM-2975 exposure (31–57%) (Fig. 4E and F).

BAD and SRM-2975 induce inflammatory responses

IL-8, IL-10 and TNF-α were measured in U937 supernatants following 24 h challenges with BAD or SRM-2975. Compared with the particle-free control, BAD exposure significantly increased IL-8 secretion by 41–120% from concentrations ≥4 μg ml^{-1} ($p \leq 0.01$ to < 0.001) and IL-10 secretion by 145–185% at concentrations ≥14 μg ml^{-1} ($p \leq 0.01$ to <0.001) (Fig. 5A and E). SRM-2975 also induced significant increases in IL-8 secretion (60–130%, $p \leq 0.001$) from concentrations ≥4 μg ml^{-1} (Fig. 5B). IL-10 secretion increased in a dose-dependent manner following exposure to SRM-2975, reaching statistical significance at 25 μg ml^{-1} (116% greater than control, $p \leq 0.05$) (Fig. 5F). SRM-2975 challenge at 4–25 μg ml^{-1} significantly increased TNF-α secretion by 38, 68, 50 and 76% in comparison to the particle-free control ($p \leq 0.01$, 0.001, 0.001 and 0.001 respectively) (Fig. 5D) but BAD exposure only induced significant increases in TNF-α secretion at the 25 μg ml^{-1} doses (55% higher than control, $p \leq 0.01$) (Fig. 5C). Where cells were exposed to equivalent particle doses in the presence of DFO, secretion of pro-inflammatory IL-8 was inhibited and remained equivalent to the particle-free control (ESI,† Fig. S3A and B). In contrast, the secretion of TNF-α that accompanied high-dose BAD exposure was not altered by the presence of DFO and elevated IL-10 secretion was still evident

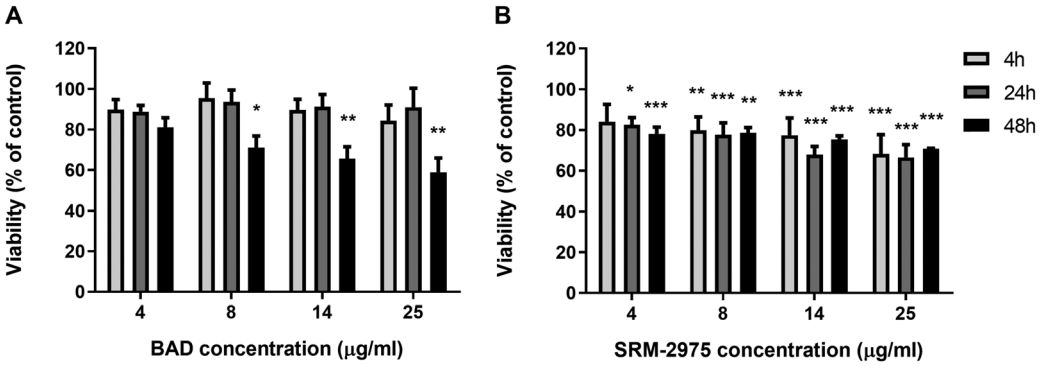

Fig. 3 Viability of U937 cells following 4–48 h exposures to 4–25 μg ml^{-1} BAD (A) or SRM-2975 (B). Values are displayed as percentages of a particle-free control and represent the mean ± SE of 6 individual measurements, each consisting of 4 technical replicates. Significant differences in viability were determined *via* one-way ANOVA tests with Bonferroni correction. *$p \leq 0.05$, **$p \leq 0.01$, ***$p \leq 0.00$.

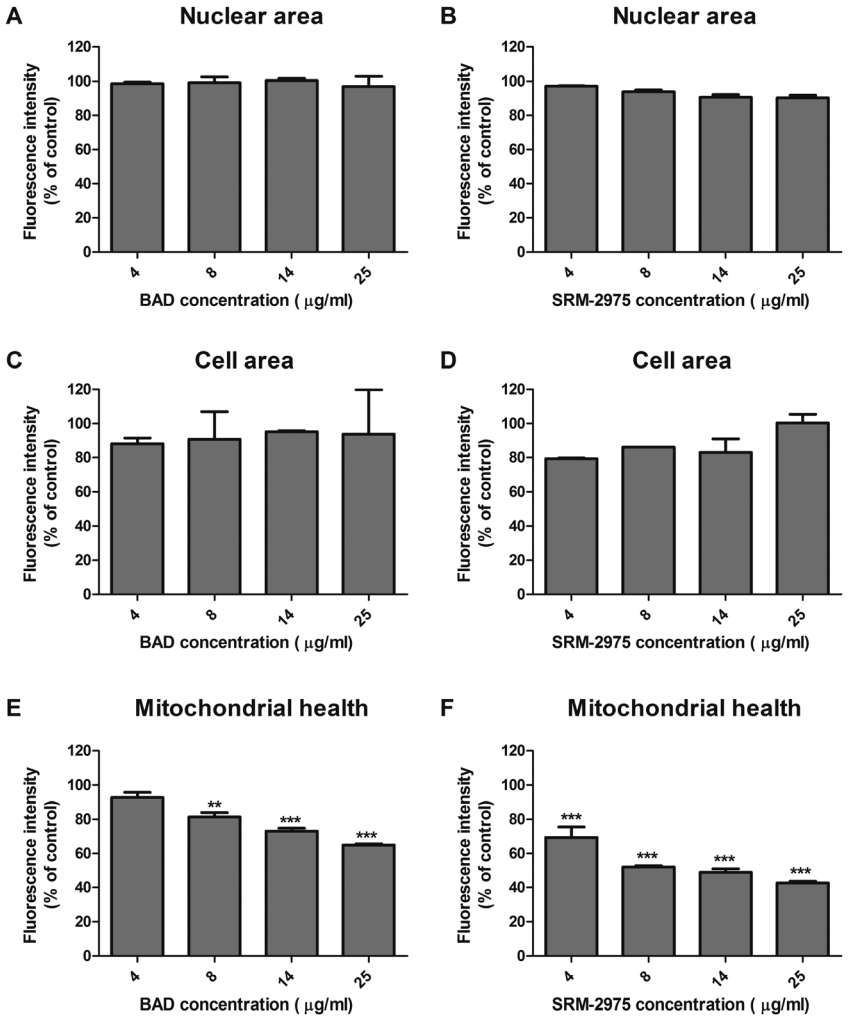

Fig. 4 Fluorescent intensities of Hoechst nuclear stain (A and B) CellMask Deep Red cytoplasmic stain (C and D) and Mitotracker Red stain for intact mitochondrial membrane potential (E and F) in U937s after 24 h exposure to 4–25 μg ml^{-1} BAD or SRM-2975. Fluorescent intensities (mean ± SE of independent measurements) were determined using an IN Cell Analyzer 6000 and are displayed as a percentage of a particle-free control. Significant differences in the fluorescence intensities of staining were identified between control and particle-treated cells using one-way ANOVA tests with Bonferroni correction. **$p \leq 0.01$, ***$p \leq 0.001$.

following exposure to BAD at all doses (60–105% higher than control, p = ns to <0.001) or 25 μg ml^{-1} SRM-2975 (22% higher than control, $p \leq 0.001$) (ESI,† Fig. S3E and F). When cells were incubated in particle-free media following the 24 h exposure to

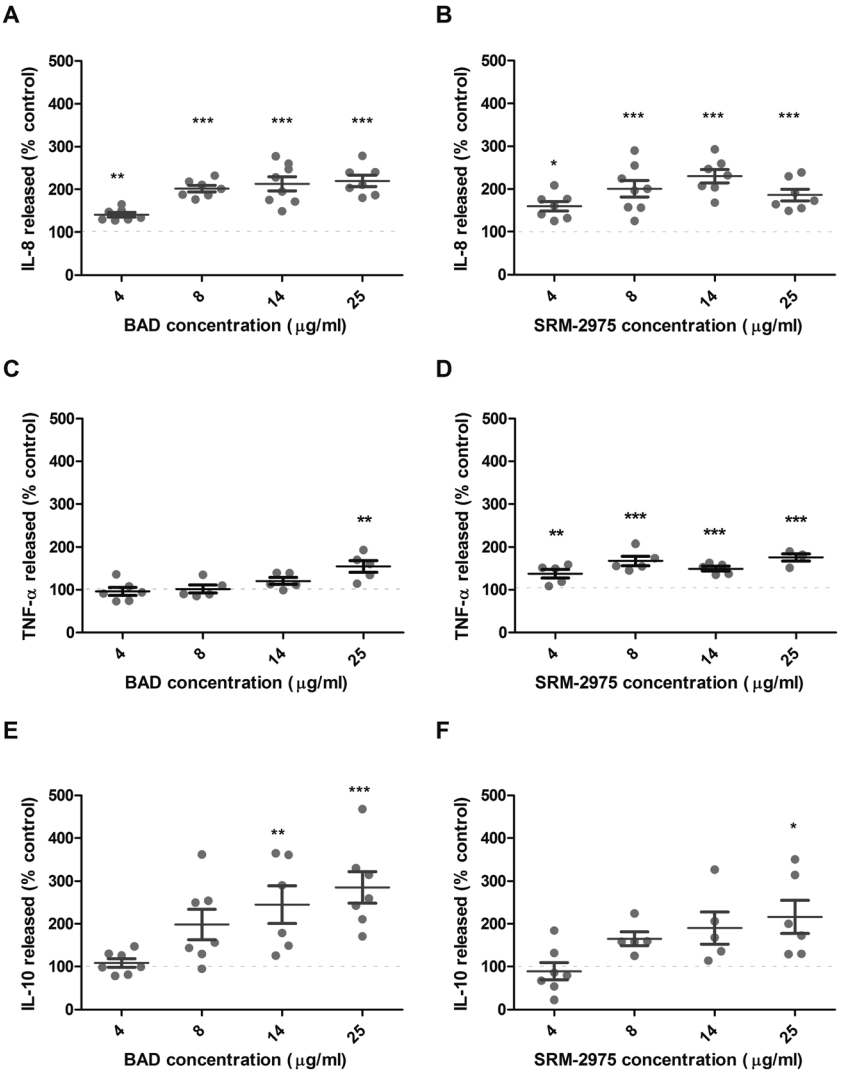

Fig. 5 Supernatant IL-8 (A and B), TNF-α (C and D) and IL-10 (E and F) concentrations derived from U937 cells after a 24 h exposure to BAD (A, C and E) and SRM-2975 (B, D and F). Values are expressed as percentages of particle-free controls and normalised to total cellular protein concentrations with error bars depicting the SE generated during 5–7 replicates. Significant differences in cytokine concentration were identified between control and particle-treated cells using one-way ANOVA tests with Bonferroni correction. *$p \leq 0.05$, **$p \leq 0.01$, ***$p \leq 0.001$.

BAD or SRM-2975, IL-8 and TNF-α concentrations returned to baseline levels (ESI,† Fig. S4A–D). In contrast, the dose-dependent increase in IL-10 concentrations after BAD challenge persisted over the recovery period, but not to a statistically significant extent (ESI,† Fig. S4E and F).

BAD and SRM-2975 inhibit phagocytic function

The impact of particle exposure on U937 function was assessed by measuring cellular capacity to ingest live *S. aureus* following treatment. After 24 h exposures to 4 and 8 μg ml^{-1} BAD, the number of *S. aureus* ingested was reduced by 30 and 29% (respectively) compared to the particle-free control ($p \leq 0.001$ and $p \leq 0.01$). When BAD dosage was increased to 14 or 25 μg ml^{-1}, the number of bacteria ingested by the macrophages was further reduced to 285 or 27% of the particle-free controls ($p \leq 0.001$) (Fig. 6A). SRM-2975 exposure induced a similar response with the 4 μg ml^{-1} treatment, reducing *S. aureus* ingestion by 44% ($p \leq 0.001$) in comparison to the particle-free control and 8, 14 and 25 μg ml^{-1} doses reducing bacterial ingestion by 52, 64 and 68%, respectively ($p \leq 0.001$) (Fig. 6B). *S. aureus* growth curves, produced in the presence or absence of BAD or SRM-2975, confirmed that these results were not caused by direct bactericidal or bacteriostatic interactions between the particles and bacteria (ESI,† Fig. S5).

In the presence of DFO, *S. aureus* uptake increased by 217 and 197% following exposure to 14 and 25 μg ml^{-1} BAD ($p \leq 0.05$) (as compared with DFO-free exposures). Similarly, DFO improved *S. aureus* uptake by 171–228% in cells treated with 4–25 μg ml^{-1} SRM-2975 ($p \leq 0.05$–0.001). For both particles, the chelator restored bacterial uptake to levels comparable to the particle-free control (Fig. 6C and D). No significant difference was found between the numbers of *S. aureus* that were ingested by particle-free control cells with and without DFO treatment, indicating that the chelator had no direct effect on phagocytosis. As well as

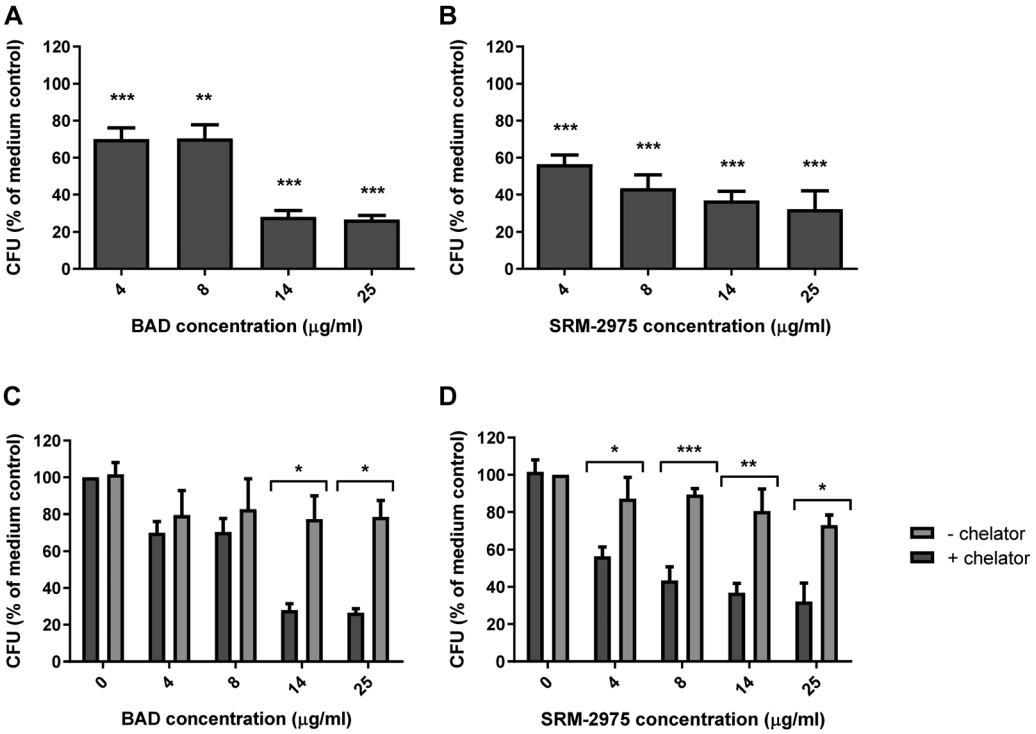

Fig. 6 Quantities of *S. aureus* ingested by U937 cells over a 2 h period subsequent to 24 h incubation with 4–25 μg ml^{-1} BAD (A) or SRM-2975 (B), 4–25 μg ml^{-1} BAD (−chelator) or 4–25 μg ml^{-1} BAD spiked with 250 μg ml^{-1} (380 μM) desferroxamine mesylate (+chelator) (C) and 4–25 μg ml^{-1} SRM-2975 (−chelator) or 4–25 μg ml^{-1} SRM-2975 spiked with 250 μg ml^{-1} desferroxamine mesylate (+chelator) (D), and 4–25 μg ml^{-1} BAD. Values were normalised to concentrations of total cellular proteins and are presented as percentages of a particle-free control and represent the mean ± SE of 4–6 biological repeats. Significant differences in CFU were identified between control and particle-treated cells using one-way ANOVA tests with Bonferroni correction and between cells treated with particles with or without desferroxamine using two-way ANOVA tests with Bonferroni correction. *$p \leq 0.05$, **$p \leq 0.01$, ***$p \leq 0.001$.

metals, particulate toxicity has been attributed to surface-bound bacterial endotoxins and PAHs.[36] We therefore examined the impact of 24 h exposures to 1 μg ml^{-1} LPS or 1 μg ml^{-1} benzopyrene on the phagocytic activity of U937 cells. While LPS induced a significant decrease in the number of *S. aureus* that the U937s ingested (14%, $p \leq 0.05$), benzopyrene did not decrease phagocytic behaviour to a significant extent (ESI,† Fig. S6).

Finally, we examined the capacity of U937s to recover their phagocytic capacity after acute particulate challenge. Cells were exposed to particles for 24 h, then incubated with particle-free medium for a further 24 h before phagocytic capacity was quantified. For both particles, phagocytic capacity was restored, exhibiting no significant differences to particle-free controls (Fig. 7A and B).

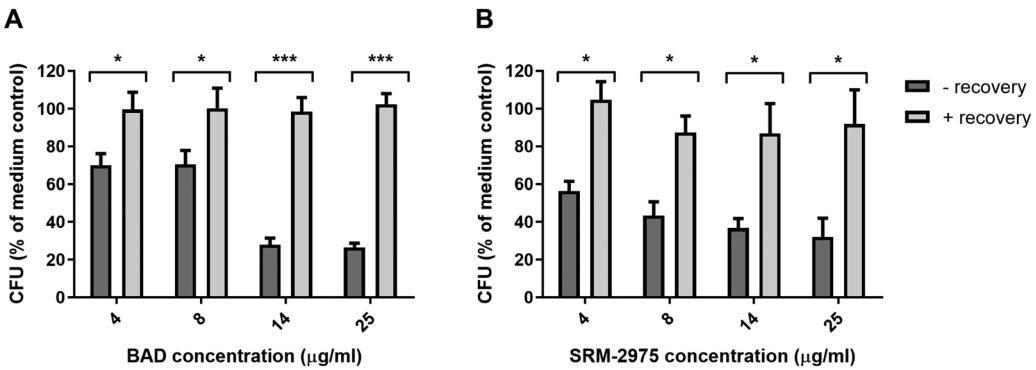

Fig. 7 Quantities of *S. aureus* ingested by U937s over a 2 h period subsequent to 24 h incubation with 4–25 μg ml^{-1} BAD (A) or SRM-2975 (B) then 24 h incubation in particle-free media. Values were normalised to concentrations of total cellular proteins and are presented as percentages of a particle-free control and represent the mean ± SE of 4–6 biological repeats. Significant differences in CFU were identified between particle-treated and particle rested cells using two-way ANOVA tests with Bonferroni correction. *$p \leq 0.05$, ***$p \leq 0.001$.

Discussion

Using a U937 human macrophage model, we compared the toxicity of two compositionally distinct contributors to traffic-derived pollution; tailpipe-derived particulate matter from diesel engines (SRM-2975) and vehicle-derived particles from a non-tailpipe source (BAD). Trace analysis by ICP-MS confirmed that the metallic content of BAD was considerably greater than that of SRM-2975 and was contributed to by many more species; a signature that was reflected intracellularly in exposed macrophages. Contrary to our hypothesis however, the two particles elicited broadly equivalent cellular responses; stimulating cytokine secretion, impairing phagocytic capacity and disrupting mitochondrial integrity at sub-lethal doses. For both particle types, heightened IL-8 and TNF-α secretion as well as impairment of phagocytic capacity were abolished by the presence of the metal chelator, DFO, suggesting that these effects were dependent on PM metal content. Together, these data demonstrate that both DEP and BAD can perturb cell function. Consequently, it may be necessary to regulate emissions of both particle types to protect public health.

Impacts of particles on mitochondrial function

Previous studies have implicated oxidative potential as a key contributor to particulate toxicity, with intracellular ROS generation associating with mitochondrial dysfunction in A549 alveolar epithelial cells and THP-1 macrophages following exposure to diesel exhaust particles[37] and diesel exhaust organic extracts.[38] Similarly, we observed a dose dependent decrease in mitochondrial membrane integrity following exposure to SRM-2975 or BAD particles (Fig. 4). This finding is consistent with the work of Karlsson *et al.* (2008) who demonstrated that mitochondrial depolarisation occurred in A549 pulmonary epithelial cells following 8 h challenges by PM_{10} samples (40 μg cm^{-2}) that were collected from a subway and street location in Stockholm.[39] Despite differences in the length and strength of our exposures, it is important to note that Karlsson *et al.*'s samples included metals derived from vehicle and road/rail surface abrasion dusts.[11] Although cell death is a typical outcome of mitochondrial dysfunction, this occurred in the absence of morphometric evidence of cell swelling (a marker of necrosis), or nuclear condensation (apoptosis)[40] for both particles. SRM-2975 exposure was however, accompanied by dose-dependent losses in metabolic activity at the 24 h time-point, an effect that was present from 4 h but did not develop until later in the time-course where cells were exposed to BAD (Fig. 3). It is possible that this may be the outcome of differences in particle composition-with SRM-2975 containing greater quantities of (or more potent) components that impair mitochondrial oxidoreductase activity and resulting in a more acute response – but **Caution** must be taken when interpreting the result. Both Fe and Cu oxides (but not TiO_2) induce acute respiratory burst events in macrophages that have been exposed to concentrations as low as 20 μg ml^{-1} [41] and the respiratory burst has been demonstrated to create spikes in MTT assay signals.[42] Considering that BAD contains noteworthy quantities of both Fe and Cu ions, it is possible that ongoing ROS production masked loss of mitochondrial metabolic functions in the macrophages at the earlier time-points.

Inflammatory responses

Incubation with both BAD and SRM-2975 elicited significant increases in IL-8 production at concentrations ≥ 4 μg ml^{-1} (Fig. 5). These data are in line with evidence that both diesel and ambient particulate matter samples induce pro-inflammatory responses in both macrophages[22,43] and human bronchial epithelial cells[44,45] and is consistent with *in vivo* evidence from human challenge studies to diesel exhaust,[46] or concentrated ambient particles.[47] The pro-inflammatory potential of BAD at non-lethal dosages has previously been demonstrated using A549 and Calu-3 epithelial cells[19,20] and similar responses have been reported in primary bronchial epithelial cells challenged with metal-rich PM collected from an underground railway station.[48] Our particle-induced increases in IL-8 were inhibited when cells were exposed to BAD or DEP in the presence of DFO; a broad-range metal ion chelator, indicating that this aspect of the pro-inflammatory response was attributable to the metal/metalloid content of the particles. This conclusion is supported by the work of Gerlofs-Nijland *et al.* who demonstrated that the ability of BAD to induce Keratinocyte Chemoattractant and Macrophage-Inflammatory Protein-2 secretion into rat BALF, relative to DEP, depended on the metallic content of the particles. Here, BAD obtained from low and semi-metallic brake pad PM (composed primarily of Fe, the major component of our BAD sample) demonstrated similar potencies to DEP while NAO brake pad PM (rich in Cu, Ti, Al and Ba) caused considerably stronger inflammatory responses than DEP.[21]

It must be considered however, that additional particle components could have contributed to the pro-inflammatory response to the particles. While TNF-α concentrations were elevated at the 4 μg ml^{-1} dose for the diesel samples, a considerably greater dose of metallic BAD (25 μg ml^{-1}) was required to cause significant increases in TNF-α secretion (Fig. 5), suggesting that induction of this cytokine is more sensitive to DEP-associated components such as PAHs or carbon than it is metals. Chen *et al.* documented induction of TNF-α expression alongside mitochondrial membrane dysfunction and inhibition of phagocytic capacity in RAW 264.7 MDM following comparable exposures to TiO_2 nanoparticles (10 μg ml^{-1} for 24 h)[28] but despite documenting similar toxicity profiles for our particles and considering that DFO binds tightly with titanium(IV)[49] we did not see reductions in TNF-α secretion upon addition of the chelator for either particle. Similarly, DFO did not impair the significant increases in anti-inflammatory IL-10 secretion that were observed following exposure to BAD or SRM-2975 (Fig. 5 and ESI,† Fig. S3). Importantly, we noted that the particle-driven induction of pro-inflammatory cytokines was transient, with levels of IL-8 and TNF-α returning to control levels 24 h after particle exposure was ceased, whilst the anti-inflammatory IL-10 response persisted.

Impacts of particles on bacterial phagocytosis

One of our main interests was to determine whether BAD exposure impacts upon pulmonary immune defences. We found

that exposure to BAD or SRM 2975 significantly reduced the ability of U937s to ingest *S. aureus*, even at particle concentrations as low as 4 μg ml^{-1}. As phagocytosis by macrophages is a primary mechanism by which the lung is protected from pathogenic material, inhibition of this function could increase the susceptibility of the airway to infection, as has been previously proposed.[50] Consistent with our findings, ambient $PM_{2.5}$ and $PM_{0.1}$, metallic nanoparticles and DEP have been shown to reduce the capacity for macrophages to phagocytose respiratory pathogens.[29,51–53] In addition, a number of experimental and clinical studies (reviewed extensively by Brugha *et al.*[54]) have shown that urban air pollution and household air pollution[55] as well as exposure to electronic cigarette smoke disrupts pulmonary innate immune defences and increases susceptibility to bacterial and viral infections.[56,57]

Interestingly, our study demonstrated that impairment of phagocytic activity could be restored by: (i) letting the cells recover for 24 h in particulate-free cell culture media and (Fig. 7) ((ii) the presence of a metal chelator (Fig. 6C and D). Similar results were observed by Zhou *et al.* (2007) who found that iron chelation reversed ambient PM-induced inhibition of bacterial internalisation.[53] Influencing our considerations of how particle-derived metal species might disrupt phagocytosis, Chen *et al.*'s study of TiO_2 nanoparticle exposure indicated that particle-mediated loss of *E. coli* uptake is accompanied by disruption of proteins required for key phagocytic processes including cytoskeletal reorganisation, endocytosis and ATP production.[28] As well as metals, the toxicity of traffic-related PM has been related to its content of endotoxins such as LPS and polycyclic aromatic hydrocarbons, which are capable of exacerbating oxidative stress and inflammation in the lung.[58] As SRM-2975 is rich in PAHs, including benzopyrene,[59] we investigated whether this PAH, would impair bacterial phagocytosis yet found no supportive evidence (ESI,† Fig. S6). In contrast, LPS induced a significant decrease in phagocytic capability (ESI,† Fig. S6), though minimal compared with the metal-dependent effect. Together, our findings highlight the importance of monitoring and regulating non-tailpipe emissions (especially those with metallic compositions), which in contrast to tailpipe emissions, are not yet monitored by European and US EPA directives.

Dissecting out metal contributions to the observed responses

The capacity of DFO to significantly inhibit both the induction of the pro-inflammatory cytokine release (IL-8) and the particle-induced impairment of phagocytosis was unexpected, given that the diesel particulate was largely devoid of pro-oxidant metals, such as Fe, Cu, or metals known to perturb intracellular redox indirectly, such as Zn. We therefore focused on the potential role of the metals common to both particle types (As, Ti, V and Sb), where we could demonstrate: (a) broadly equivalent concentrations; (b) literature-based evidence of their effective chelation by desferroxamine, and (c) evidence that the metals where taken up into the cultured cells. Based on these criteria, we did not consider antimony (Sb) further, due to its elevated concentration in BAD and lack of evidence of intra-cellular accumulation. Each of the remaining metals demonstrated increased intra-cellular concentrations 24 h post challenge, but only vanadium provided a clear dose dependent relationship with the two particle types. In the present study we lack information on metal speciation, but upon cellular uptake, vanadium in the 4+ oxidation state, vanadyl, has been shown to be the predominate form.[60] Supporting our focus on this metal, vanadyl has been shown to form bi-tetra and hexadenate-bonded complexes with DFO when examined in a cell-free acidic medium;[61] interactions that could underlie DFO-induced reductions in tissue accumulation and increases in fecal, urinary and biliary excretion of vanadyl ions in rats following exposure to 48VOSO4.[62,63]

Whilst exposures of rat liver microsomes to vanadate have implicated oxidative stress as a mechanism by which vanadium exposure causes toxicity,[64] it seems unlikely that this would be the dominant mode of action for both of our model particles, as BAD contained considerably higher content of other well established metal ROS catalysts.[65] Vanadate and vanadyl also act as phosphate analogues, interfering with a range of phosphate dependent enzymes, including Na^+K^+ATPase, Ca^{++} ATPase, and the dynein ATPase[66] and potently inhibit phosphatases,[67] resulting in the activation of kinase stress pathways. However, as Zn, also an established phosphatase inhibitor[68] was present at greater concentration in BAD and previous studies have indicated that Zn(II) is a more effective phosphatase inhibitor than vanadyl or As (in sodium arsenite form),[69] again this does not seem a plausible mechanism.

There is also evidence that the vanadium compound, sodium orthovanadate, can activate Ca^{++}-dependent cytoplasmic phospholipase A2, resulting in the enhanced production of arachidonic acid metabolites.[70] Interestingly, previous work examined the inflammatory responses of murine RAW264.7 cells to ambient PM samples demonstrated a correlation between PM metal content and the release of arachidonic acid, which was inhibited with the use of the metal chelator diethylenetriaminepentaacetic acid.[22] Vanadyl, vanadate, bis(acetylacetonato)oxovanadium and vanadium citrate have also been shown to interact directly with isolated mitochondria, disrupting membrane potential and enhancing intracellular ROS production.[71] Thus, PM-associated vanadium has the potential to perturb cell function.

Much of the evidence base examining the airway toxicity of titanium is based on occupational exposures to wielding fume, or increasingly from studies investigating nano TiO_2. Exposure to welding fume has been associated with increased susceptibility of welders to pneumococcal pneumonia, with the underlying mechanism related to increased binding and uptake of bacteria into human bronchial epithelial cells. However, the extent to which this can be attributed to Ti in a compositional complex dust (rich in Fe) is difficult to dissect out.[72] Nanosize TiO_2 has been demonstrated to elicit oxidative stress and the release of pro-inflammatory mediators in human primary epithelial cells,[73] as well as increase the susceptibility of the murine lung to pneumonia.[74] Therefore, a role for PM associated Ti in the responses observed with BAD and SRM 2975 cannot be excluded, but again, must be viewed in the context of

higher abundance of redox active metals in the BAD samples. The role of As compounds and its major metabolites in inducing cytotoxicity and increased susceptibility to infection in pulmonary models has yielded ambiguous results to date.[75]

Limitations of the study

SRM-2975 was chosen as a comparator for BAD because it has been used in many previous studies of DEP toxicity and its effects on pulmonary cells are well characterised *in vitro*. However, the sample originates from the engine of an industrial forklift truck, prior to recent developments in filter technology and exhaust after-treatment,[76] making it poorly representative of current road traffic-related DEP emissions. In contrast, the BAD sample included material from a mixture of commercial vehicles, produced by currently popular manufacturers, thus representing a more timely and realistic human exposure scenario. Humans would inhale BAD from a combination of vehicle models and brake pad compositions rather than from isolated types. It is important to consider however, that this method of BAD particle collection has not been standardised. Proposals for common sampling and assessment of brake wear are still under development by the Particle Measurement Group of the United Nations Economic Commission for Europe particles.[77]

Conclusions

To summarise, we have identified that two major contributors to traffic-related PM; BAD and DEP, exert similar adverse effects on human macrophage function, despite possessing significant compositional differences. The capacity of both particles to impair bacterial phagocytosis is especially pertinent as this is consistent with increased susceptibility to airway infection. Of great importance is the observation that metals are key drivers of this toxicity, even in particle species that possess relatively low metal concentrations, as this indicates that other uncharacterised traffic-derived particles could be contributing to adverse respiratory health. Currently, regulations target tailpipe emissions alone but these data imply that traffic-related abrasion particles are equally capable of harming pulmonary cells. Therefore, we believe that future pollution mitigation strategies will need to consider additional vehicle-derived sources if the full benefit to public health is to be achieved.

Funding

Liza Selley was supported by the Integrative Toxicology Training Partnership (ITTP) from the Medical Research Council, UK (Grant awarded to TG and TA) and a Mini Fellowship grant awarded by the *In Vitro* Toxicology Society, UK. TG was supported by the National Institute for Health Research Health Protection Research Unit (NIHR HPRU) in Health Impact of Environmental Hazards held at King's College London in partnership with Public Health England (PHE) and Imperial College London. Our metal analysis was performed by the London Metallomics Facility and funded by the Wellcome trust (grant reference 202902/Z/16/Z, awarded to IM).

Author's contributions

LSE: experimental design, experimental work (cell culture, cells challenges, high content screening, immunoassays, functional assays of phagocytosis, particle sizing), data analysis, manuscript preparation and corresponding author; LSC: experimental design, experimental work (as for LSE) data analysis (equal contribution with LSE) and manuscript preparation; HM: experimental design and manuscript preparation; TF: experimental work (cell culture, cell challenges, immunoassays, functional assays of phagocytosis); BF: experimental design, data interpretation and manuscript preparation; TWG: experimental design, data interpretation and manuscript preparation; TS: provision of brake dust samples and manuscript preparation; NC: particle extractions of oxidative potential determinations; TJA: experimental design, data interpretation and manuscript preparation; IM: study design, metal analysis, data analysis and interpretation and manuscript preparation; AK: lead author, study design, coordination of the experimental work, high content screening work, data analysis and interpretation, manuscript preparation.

Abbreviations

AA	Ascorbic acid
ANOVA	Analysis of variance
BALF	Bronchoalveolar lavage fluid
BAD	Brake abrasion dust
BCA	Bicinchoninic acid
CFU	Colony forming units
CM	Cell culture media
CV	Commercial vehicle
DFO	Desferroxamine
DEP	Diesel exhaust particle
DLS	Dynamic light scattering
ELISA	Enzyme linked immunosorbent assay
GSH	Glutathione (reduced)
ICP-MS	Inductively coupled plasma-mass spectrometry
IL-8	Interleukin-8
IL-10	Interleukin-10
LPS	Lipopolysaccharide
MHB	Mueller Hinton broth
MDM	Monocyte-derived macrophages
MTT	3-(4,5-dimethylthiazol-2-yl)-2,5-diphenyl tetrazolium bromide
NAO	Non-asbestos organic
PDI	Polydispersity index
PM	Particulate matter
PM_{10}	Particulate matter up to 10 μm in diameter
$PM_{2.5}$	Particulate matter up to 2.5 μm in diameter
PMA	Phorbol 12-myristate 13-acetate
PAH	Polyaromatic hydrocarbons
PBS	Phosphate buffered saline

PDI	Polydispersity indices
ROS	Reactive oxygen species
RTLF	Respiratory tract lining fluid
SE	Standard error of the mean
SEM	Scanning electron microscopy
SRM-2975	Standard reference material 2975
S. aureus	Staphylococcus aureus
TNF-α	Tumour necrosis factor-α

Conflicts of interest

The authors declare that they have no competing interests.

Acknowledgements

The authors would like to thank SMP Svensk Maskinprovning, Sweden for providing the brake abrasion dust employed in this study. The authors would also like to acknowledge Stevenage Bioscience Catalyst, GlaxoSmithKline and GE Healthcare for providing access to the IN Cell Analyzer 6000 and for training on the instrument. LSE acknowledges the MRC Integrative Toxicology Training Partnership (ITTP) and the *In Vitro* Toxicology Society for financial support.

References

1 HEI (HEI), Traffic-Related Air Pollution: A Critical Review of the Literature on Emissions, Exposure, and Health Effects. Boston, USA, 2010.

2 W. J. Gauderman, R. Urman, E. Avol, K. Berhane, R. McConnell and E. Rappaport, *et al.*, Association of improved air quality with lung development in children, *N. Engl. J. Med.*, 2015, **372**(10), 905–913.

3 C. Freire, R. Ramos, R. Puertas, M.-J. Lopez-Espinosa, J. Julvez and I. Aguilera, *et al.*, Association of traffic-related air pollution with cognitive development in children, *J. Epidemiol. Community Health*, 2010, **64**(3), 223–228.

4 T. Grigoratos and G. Martini, Brake wear particle emissions: a review, *Environ Sci. Pollut. Res. Int.*, 2015, **22**(4), 2491–2504.

5 R. W. Atkinson, A. Analitis, E. Samoli, G. W. Fuller, D. C. Green and I. S. Mudway, *et al.*, Short-term exposure to traffic-related air pollution and daily mortality in London, UK, *J. Exposure Sci. Environ. Epidemiol.*, 2016, **26**(2), 125–132. Available from: http://www.ncbi.nlm.nih.gov/pubmed/26464095.

6 N. A. H. Janssen, G. Hoek, M. Simic-Lawson, P. Fischer, L. van Bree and H. ten Brink, *et al.*, Black Carbon as an Additional Indicator of the Adverse Health Effects of Airborne Particles Compared with PM10 and PM2.5, *Environ. Health Perspect.*, 2011, **119**(12), 1691–1699. Available from: http://www.ncbi.nlm.nih.gov/pubmed/21810552.

7 R. N. Bauer, D. Diaz-Sanchez and I. Jaspers, Effects of air pollutants on innate immunity: the role of Toll-like receptors and nucleotide-binding oligomerization domain-like receptors, *J. Allergy Clin. Immunol.*, 2012, **129**(1), 14–24, quiz 25–26. Available from: http://www.ncbi.nlm.nih.gov/pubmed/22196521.

8 C. Hatzis, J. J. Godleski, B. González-Flecha, J. M. Wolfson and P. Koutrakis, Ambient Particulate Matter Exhibits Direct Inhibitory Effects on Oxidative Stress Enzymes, *Environ. Sci. Technol.*, 2006, **40**(8), 2805–2811, DOI: 10.1021/es0518732.

9 Y. Zhao, P. V. Usatyuk, I. A. Gorshkova, D. He, T. Wang and L. Moreno-Vinasco, *et al.*, Regulation of COX-2 expression and IL-6 release by particulate matter in airway epithelial cells, *Am. J. Respir. Cell Mol. Biol.*, 2009, **40**(1), 19–30.

10 R. K. Robinson, M. A. Birrell, J. J. Adcock, M. A. Wortley, E. D. Dubuis and S. Chen, *et al.*, Mechanistic link between diesel exhaust particles and respiratory reflexes, *J. Allergy Clin. Immunol.*, 2018, **141**(3), 1074–1084. Available from: https://www.sciencedirect.com/science/article/pii/S0091674917307960.

11 F. Amato, F. R. Cassee, H. A. C. Denier van der Gon, R. Gehrig, M. Gustafsson and W. Hafner, *et al.*, Urban air quality: The challenge of traffic non-exhaust emissions, *J. Hazard. Mater.*, 2014, **275**, 31–36. Available from: http://linkinghub.elsevier.com/retrieve/pii/S030438941400315X.

12 B. R. Denby, I. Sundvor, C. Johansson, L. Pirjola, M. Ketzel and M. Norman, *et al.*, A coupled road dust and surface moisture model to predict non-exhaust road traffic induced particle emissions (NORTRIP). Part 1: Road dust loading and suspension modelling, *Atmos. Environ.*, 2013, **77**, 283–300.

13 R. M. Harrison, A. M. Jones, J. Gietl, J. Yin and D. C. Green, Estimation of the Contributions of Brake Dust, Tire Wear, and Resuspension to Nonexhaust Traffic Particles Derived from Atmospheric Measurements, *Environ. Sci. Technol.*, 2012, **46**(12), 6523–6529. Available from: http://www.ncbi.nlm.nih.gov/pubmed/22642836.

14 N. Bukowiecki, R. Gehrig, P. Lienemann, M. Hill, R. Figi, B. Buchmann, *et al.*, *PM10 emission factors of abrasion particles from road traffic (APART)*, 2009. Available from: https://trimis.ec.europa.eu/sites/default/files/project/documents/20150710_141622_66365_priloha_radek_1052.pdf.

15 B. D. Garg, S. H. Cadle, P. A. Mulawa, P. J. Groblicki, C. Laroo and G. A. Parr, Brake Wear Particulate Matter Emissions, *Environ. Sci. Technol.*, 2000, **34**(21), 4463–4469, DOI: 10.1021/es001108h.

16 F. J. Kelly, Oxidative stress: its role in air pollution and adverse health effects, *Occup. Environ. Med.*, 2003, **60**(8), 612–616.

17 M. S. Happo, R. O. Salonen, A. I. Hälinen, P. I. Jalava, A. S. Pennanen and J. A. M. A. Dormans, *et al.*, Inflammation and tissue damage in mouse lung by single and repeated dosing of urban air coarse and fine particles collected from six European cities, *Inhalation Toxicol.*, 2010, 402–416.

18 M. I. Greenberg and D. Vearrier, Metal fume fever and polymer fume fever, *Clinical Toxicology. Informa Healthcare*, 2015, **53**, 195–203.

19 M. Gasser, M. Riediker, L. Mueller, A. Perrenoud, F. Blank and P. Gehr, *et al.*, Toxic effects of brake wear particles on epithelial lung cells *in vitro*, *Part. Fibre Toxicol.*, 2009, **6**, 30.

20 C. Puisney, E. K. Oikonomou, S. Nowak, A. Chevillot, S. Casale and A. Baeza-Squiban, *et al.*, Brake wear (nano)particle characterization and toxicity on airway epithelial cells in vitro, *Environ. Sci.: Nano*, 2018, **5**(4), 1036–1044. Available from: http://xlink.rsc.org/?DOI=C7EN00825B.

21 M. E. Gerlofs-Nijland, B. G. H. Bokkers, H. Sachse, J. J. E. Reijnders, M. Gustafsson and A. J. F. Boere, *et al.*, Inhalation toxicity profiles of particulate matter: a comparison between brake wear with other sources of emission, *Inhalation Toxicol.*, 2019, 1–10, DOI: 10.1080/08958378.2019.1606365.

22 C. Guastadisegni, F. J. Kelly, F. R. Cassee, M. E. Gerlofs-Nijland, N. A. H. Janssen and R. Pozzi, *et al.*, Determinants of the Proinflammatory Action of Ambient Particulate Matter in Immortalized Murine Macrophages, *Environ. Health Perspect.*, 2010, **118**(12), 1728–1734. Available from: http://www.ncbi.nlm.nih.gov/pubmed/20663738.

23 F. Kelly, H. R. Anderson, B. Armstrong, R. Atkinson, B. Barratt and S. Beevers, *et al.*, The impact of the congestion charging scheme on air quality in London. Part 2. Analysis of the oxidative potential of particulate matter, *Res. Rep. - Health Eff. Inst.*, 2011, **155**, 73–144.

24 N. Künzli, I. S. Mudway, T. Götschi, T. Shi, F. J. Kelly and S. Cook, *et al.*, Comparison of oxidative properties, light absorbance, total and elemental mass concentration of ambient PM2.5 collected at 20 European sites, *Environ. Health Perspect.*, 2006, **114**(5), 684–690.

25 M. E. Gerlofs-Nijland, J. A. M. A. Dormans, H. J. T. Bloemen, D. L. A. C. Leseman, A. John and F. Boere, *et al.*, Toxicity of coarse and fine particulate matter from sites with contrasting traffic profiles, *Inhalation Toxicol.*, 2007, **19**(13), 1055–1069.

26 J. M. Antonini and J. R. Roberts, Chromium in Stainless Steel Welding Fume Suppresses Lung Defense Responses Against Bacterial Infection in Rats, *J. Immunotoxicol.*, 2007, **4**(2), 117–127. Available from: http://www.ncbi.nlm.nih.gov/pubmed/18958720.

27 K. Palmer and D. Coggon, *Does occupational exposure to iron promote infection? Occupational and Environmental Medicine*, BMJ Publishing Group, 1997, vol. 54, pp. 529–534.

28 Q. Chen, N. Wang, M. Zhu, J. Lu, H. Zhong and X. Xue, *et al.*, TiO_2 nanoparticles cause mitochondrial dysfunction, activate inflammatory responses, and attenuate phagocytosis in macrophages: A proteomic and metabolomic insight, *Redox Biol.*, 2018, **15**, 266–276. Available from: http://www.ncbi.nlm.nih.gov/pubmed/29294438.

29 L. K. Braydich-Stolle, J. L. Speshock, A. Castle, M. Smith, R. C. Murdock and S. M. Hussain, Nanosized Aluminum Altered Immune Function, *ACS Nano*, 2010, **4**(7), 3661–3670. Available from: http://www.ncbi.nlm.nih.gov/pubmed/20593840.

30 N. Vichit-Vadakan, B. D. Ostro, L. G. Chestnut, D. M. Mills, W. Aekplakorn and S. Wangwongwatana, *et al.*, Air pollution and respiratory symptoms: results from three panel studies in Bangkok, Thailand, *Environ. Health Perspect.*, 2001, **109**(Suppl 3), 381–387. Available from: http://www.ncbi.nlm.nih.gov/pmc/articles/PMC1240555/.

31 S. G. Kumar, A. Majumdar, V. Kumar, B. N. Naik, K. Selvaraj and K. Balajee, Prevalence of acute respiratory infection among under-five children in urban and rural areas of puducherry, India, *J. Nat. Sci., Biol. Med.*, 2015, **6**(1), 3–6. Available from: http://www.ncbi.nlm.nih.gov/pubmed/25810626.

32 L. Miyashita, R. Suri, E. Dearing, I. Mudway, R. E. Dove and D. R. Neill, *et al.*, E-cigarette vapour enhances pneumococcal adherence to airway epithelial cells, *Eur. Respir. J.*, 2018, **51**(2), 1701592. Available from: http://www.ncbi.nlm.nih.gov/pubmed/29437942.

33 I. S. Mudway, N. Stenfors, A. Blomberg, R. Helleday, C. Dunster and S. L. Marklund, *et al.*, Differences in basal airway antioxidant concentrations are not predictive of individual responsiveness to ozone: a comparison of healthy and mild asthmatic subjects, *Free Radical Biol. Med.*, 2001, **31**(8), 962–974.

34 A. Kumar, W. Terakosolphan, M. Hassoun, K.-K. Vandera, A. Novicky and R. Harvey, *et al.*, A Biocompatible Synthetic Lung Fluid Based on Human Respiratory Tract Lining Fluid Composition, *Pharm. Res.*, 2017, **34**(12), 2454–2465. Available from: http://www.ncbi.nlm.nih.gov/pubmed/28560698.

35 P. Singh, D. M. DeMarini, C. A. J. Dick, D. G. Tabor, J. V. Ryan and W. P. Linak, *et al.*, Sample characterization of automobile and forklift diesel exhaust particles and comparative pulmonary toxicity in mice, *Environ. Health Perspect.*, 2004, **112**(8), 820–825. Available from: http://www.ncbi.nlm.nih.gov/pubmed/15175167.

36 J. G. Ayres, P. Borm, F. R. Cassee, V. Castranova, K. Donaldson and A. Ghio, *et al.*, Evaluating the Toxicity of Airborne Particulate Matter and Nanoparticles by Measuring Oxidative Stress Potential—A Workshop Report and Consensus Statement, *Inhalation Toxicol.*, 2008, 75–99.

37 K. Jantzen, M. Roursgaard, C. Desler, S. Loft, L. J. Rasmussen and P. Møller, Oxidative damage to DNA by diesel exhaust particle exposure in co-cultures of human lung epithelial cells and macrophages, *Mutagenesis*, 2012, **27**(6), 693–701.

38 T. S. Hiura, N. Li, R. Kaplan, M. Horwitz, J. C. Seagrave and A. E. Nel, The role of a mitochondrial pathway in the induction of apoptosis by chemicals extracted from diesel exhaust particles, *J. Immunol.*, 2000, **165**(5), 2703–2711.

39 H. L. Karlsson, A. Holgersson and L. Möller, Mechanisms related to the genotoxicity of particles in the subway and from other sources, *Chem. Res. Toxicol.*, 2008, **21**(3), 726–731.

40 E. Hoffman, A. Kumar, V. Kanabar, M. Arno, L. Preux and V. Millar, *et al.*, *In Vitro* Multiparameter Assay Development Strategy toward Differentiating Macrophage Responses to Inhaled Medicines, *Mol. Pharmaceutics*, 2015, **12**(8), 2675–2687.

41 D. Breznan, P. Goegan, V. Chauhan, S. Karthikeyan, P. Kumarathasan and S. Cakmak, *et al.*, Respiratory burst in alveolar macrophages exposed to urban particles is not a predictor of cytotoxicity, *Toxicol. In Vitro*, 2013, **27**(4), 1287–1297.

42 S. B. Pruett and A. Y. Loftis, Characteristics of MTT as an indicator of viability and respiratory burst activity of human neutrophils, *Int. Arch. Allergy Appl. Immunol.*, 1990, **92**(2), 189–192.

43 N. Li, S. Kim, M. Wang, J. Froines, C. Sioutas and A. Nel, Use of a stratified oxidative stress model to study the biological effects of ambient concentrated and diesel exhaust particulate matter, *Inhalation Toxicol.*, 2002, **14**(5), 459–486.

44 P. A. Steerenberg, J. A. Zonnenberg, J. A. Dormans, P. N. Joon, I. M. Wouters and L. van Bree, *et al.*, Diesel exhaust particles induced release of interleukin 6 and 8 by (primed) human bronchial epithelial cells (BEAS 2B) *in vitro*, *Exp. Lung Res.*, 1997, **24**(1), 85–100.

45 B. Hawley, D. McKenna, A. Marchese and J. Volckens, Time course of bronchial cell inflammation following exposure to diesel particulate matter using a modified EAVES, *Toxicol. In Vitro*, 2014, **28**(5), 829–837.

46 A. F. Behndig, I. S. Mudway, J. L. Brown, N. Stenfors, R. Helleday and S. T. Duggan, *et al.*, Airway antioxidant and inflammatory responses to diesel exhaust exposure in healthy humans, *Eur. Respir. J.*, 2006, **27**(2), 359–365.

47 J. M. Samet, A. Rappold, D. Graff, W. E. Cascio, J. H. Berntsen and Y.-C. T. Huang, Concentrated ambient ultrafine particle exposure induces cardiac changes in young healthy volunteers, *Am. J. Respir. Crit. Care Med.*, 2009, **179**(11), 1034–1042.

48 M. Loxham, M. J. Cooper, M. E. Gerlofs-Nijland, F. R. Cassee, D. E. Davies and M. R. Palmer, *et al.*, Physicochemical characterization of airborne particulate matter at a mainline underground railway station, *Environ. Sci. Technol.*, 2013, **47**(8), 3614–3622.

49 K. E. Jones, K. L. Batchler, C. Zalouk and A. M. Valentine, Ti(IV) and the Siderophore Desferrioxamine B: A Tight Complex Has Biological and Environmental Implications, *Inorg. Chem.*, 2017, **56**(3), 1264–1272. Available from: https://pubs.acs.org/doi/10.1021/acs.inorgchem.6b02399.

50 R. E. Brugha, N. Mushtaq, T. Round, D. H. Gadhvi, I. Dundas and E. Gaillard, *et al.*, Carbon in airway macrophages from children with asthma, *Thorax*, 2014, **69**(7), 654–659.

51 V. Kodali, M. H. Littke, S. C. Tilton, J. G. Teeguarden, L. Shi and C. W. Frevert, *et al.*, Dysregulation of macrophage activation profiles by engineered nanoparticles, *ACS Nano*, 2013, **7**(8), 6997–7010.

52 X. J. Yin, C. C. Dong, J. Y. C. Ma, J. R. Roberts, J. M. Antonini and J. K. H. Ma, Suppression of Phagocytic and Bactericidal Functions of Rat Alveolar Macrophages by the Organic Component of Diesel Exhaust Particles, *J. Toxicol. Environ. Health, Part A*, 2007, **70**(10), 820–828. Available from: http://www.ncbi.nlm.nih.gov/pubmed/17454558.

53 H. Zhou and L. Kobzik, Effect of concentrated ambient particles on macrophage phagocytosis and killing of Streptococcus pneumoniae, *Am. J. Respir. Cell Mol. Biol.*, 2007, **36**(4), 460–465. Available from: http://www.ncbi.nlm.nih.gov/pubmed/17079778.

54 R. Brugha and J. Grigg, Urban Air Pollution and Respiratory Infections, *Paediatr Respir Rev.*, 2014, **15**(2), 194–199.

55 J. Rylance, D. G. Fullerton, J. Scriven, A. N. Aljurayyan, D. Mzinza and S. Barrett, *et al.*, Household Air Pollution Causes Dose-Dependent Inflammation and Altered Phagocytosis in Human Macrophages, *Am. J. Respir. Cell Mol. Biol.*, 2015, **52**(5), 584–593.

56 T. E. Sussan, S. Gajghate, R. K. Thimmulappa, J. Ma, J.-H. Kim and K. Sudini, *et al.*, Exposure to Electronic Cigarettes Impairs Pulmonary Anti-Bacterial and Anti-Viral Defenses in a Mouse Model, ed. D. W. Metzger, *PLoS One*, 2015, **10**(2), e0116861.

57 J. H. Hwang, M. Lyes, K. Sladewski, S. Enany, E. McEachern and D. P. Mathew, *et al.*, Electronic cigarette inhalation alters innate immunity and airway cytokines while increasing the virulence of colonizing bacteria, *J. Mol. Med.*, 2016, **94**(6), 667–679.

58 F. J. Kelly and J. C. Fussell, Size, source and chemical composition as determinants of toxicity attributable to ambient particulate matter, *Atmos. Environ.*, 2012, **60**, 504–526.

59 A. Kocbach, Y. Li, K. E. Yttri, F. R. Cassee, P. E. Schwarze and E. Namork, Physicochemical characterisation of combustion particles from vehicle exhaust and residential wood smoke, *Part. Fibre Toxicol.*, 2006, **3**, 1.

60 M. Ding, P. M. Gannett, Y. Rojanasakul, K. Liu and X. Shi, One-electron reduction of vanadate by ascorbate and related free radical generation at physiological pH, *J. Inorg. Biochem.*, 1994, **55**(2), 101–112.

61 I. Batinic-Haberle, M. Birus and M. Pribanic, Siderophore chemistry of vanadium. Kinetics and equilibrium of interaction between vanadium(IV) and desferrioxamine B in aqueous acidic solutions, *Inorg. Chem.*, 1991, **30**(26), 4882–4887, DOI: 10.1021/ic00026a007.

62 T. V. Hansen, J. Aaseth and J. Alexander, The effect of chelating agents on vanadium distribution in the rat body and on uptake by human erythrocytes, *Arch fur Toxikologie*, 1982, **50–50**(3–4), 195–202, DOI: 10.1007/BF00310851.

63 S. Tubafard, S. J. Fatemi, A. S. Saljooghi and M. Torkzadeh, Removal of vanadium by combining desferrioxamine and deferiprone chelators in rats, *Med. Chem. Res.*, 2010, **19**(8), 854–863, DOI: 10.1007/s00044-009-9235-3.

64 X. Shi and N. S. Dalal, Hydroxyl radical generation in the NADH/microsomal reduction of vanadate, *Free Radical Res. Commun.*, 1992, **17**(6), 369–376.

65 M. Valko, H. Morris and M. T. D. Cronin, Metals, toxicity and oxidative stress, *Curr. Med. Chem.*, 2005, **12**(10), 1161–1208.

66 B. Mukherjee, B. Patra, S. Mahapatra, P. Banerjee, A. Tiwari and M. Chatterjee, Vanadium – an element of atypical biological significance, *Toxicol. Lett.*, 2004, **150**(2), 135–143.

67 G. Huyer, S. Liu, J. Kelly, J. Moffat, P. Payette and B. Kennedy, *et al.*, Mechanism of inhibition of protein-tyrosine phosphatases by vanadate and pervanadate, *J. Biol. Chem.*, 1997, **272**(2), 843–851.

68 R. M. Phillips, L. A. Dailey, E. Bair, J. M. Samet and N. L. Allbritton, Ex vivo chemical cytometric analysis of protein tyrosine phosphatase activity in single human airway epithelial cells, *Anal. Chem.*, 2014, **86**(2), 1291–1297.

69 J. M. Samet, R. Silbajoris, W. Wu and L. M. Graves, Tyrosine phosphatases as targets in metal-induced signaling in human airway epithelial cells, *Am. J. Respir. Cell Mol. Biol.*, 1999, **21**(3), 357–364.

70 J. Korbecki, I. Baranowska-Bosiacka, I. Gutowska, K. Piotrowska and D. Chlubek, Cyclooxygenase-1 as the main source of proinflammatory factors after sodium orthovanadate treatment, *Biol. Trace Elem. Res.*, 2015, **163**(1–2), 103–111.

71 Y. Zhao, L. Ye, H. Liu, Q. Xia, Y. Zhang and X. Yang, *et al.*, Vanadium compounds induced mitochondria permeability transition pore (PTP) opening related to oxidative stress, *J. Inorg. Biochem.*, 2010, **104**(4), 371–378.

72 R. Suri, J. Periselneris, S. Lanone, P. C. Zeidler-Erdely, G. Melton and K. T. Palmer, *et al.*, Exposure to welding fumes and lower airway infection with Streptococcus pneumoniae, *J. Allergy Clin. Immunol.*, 2015, 527–534.

73 S. Sweeney, D. Berhanu, P. Ruenraroengsak, A. J. Thorley, E. Valsami-Jones and T. D. Tetley, Nano-titanium dioxide bioreactivity with human alveolar type-I-like epithelial cells: Investigating crystalline phase as a critical determinant, *Nanotoxicology*, 2015, **9**(4), 482–492.

74 S. Hashiguchi, H. Yoshida, T. Akashi, K. Komemoto, T. Ueda and Y. Ikarashi, *et al.*, Titanium dioxide nanoparticles exacerbate pneumonia in respiratory syncytial virus (RSV)-infected mice, *Environ. Toxicol. Pharmacol.*, 2015, **39**(2), 879–886.

75 E. G. Notch, B. C. Goodale, R. Barnaby, B. Coutermarsh, B. Berwin and V. F. Taylor, *et al.*, Monomethylarsonous Acid (MMAIII) Has an Adverse Effect on the Innate Immune Response of Human Bronchial Epithelial Cells to Pseudomonas aeruginosa, *PLoS One*, 2015, **10**(11), e0142392.

76 C. A. Gonzalez and R. L. Watters, *Certificate of Analysis Office of Reference Materials Certificate Revision History on Last Page*, 2013. Available from: https://www-s.nist.gov/srmors/certificates/2975.pdf.

77 Joint Research Centre, 42nd UNECE IWG PMP MEETING: Non-exhaust particle emissions. Particle Measurement Program; United Nations Economic Commission for Europe, 2017.

